Electronic Supplementary Material (ESI) for Sustainable Energy & Fuels.

Supporting Information

An efficient hybrid supercapacitor based on Zn-Mn-Ni-S@NiSe core-shell architectures

Akbar Mohammadi Zardkhoshoui* and Saied Saeed Hosseiny Davarani*

Department of Chemistry, Shahid Beheshti University, G. C., 1983963113, Evin, Tehran, Iran.

Corresponding authors: *Tel: +98 21 22431661; Fax: +98 21 22431661; E-mail: ss-hosseiny@sbu.ac.ir (S.S.H. Davarani); and mohammadi.bahadoran@gmail.com (A. Mohammadi Zardkhoshoui)

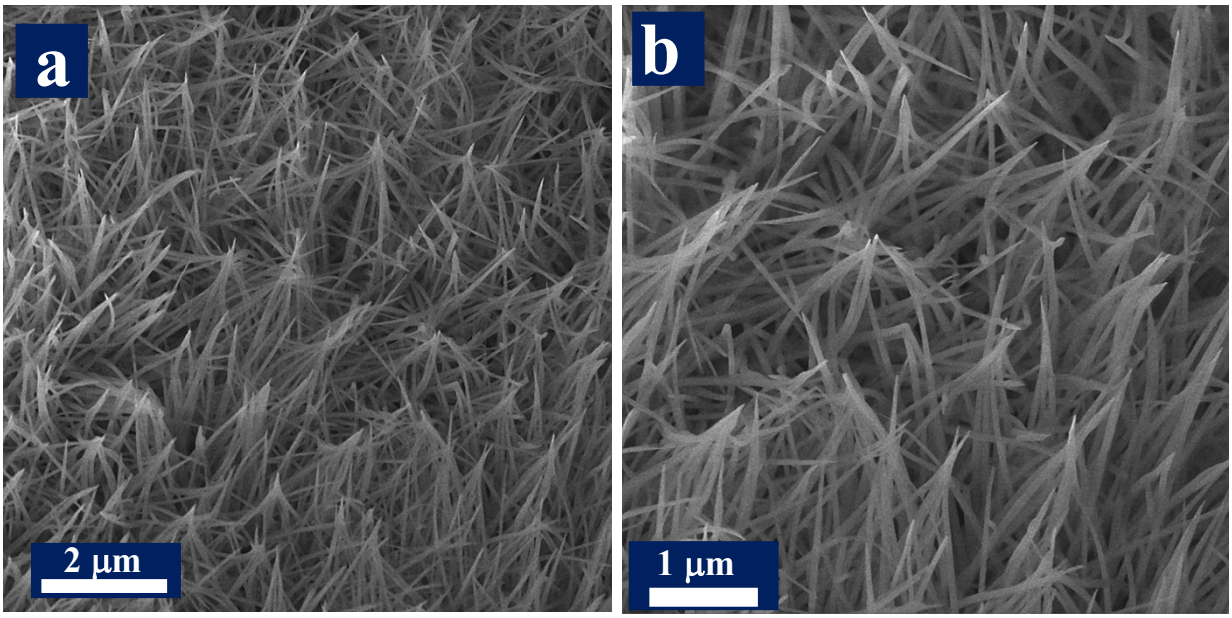

Fig. S1. FE-SEM images of the Zn-Mn-Ni-precursors.

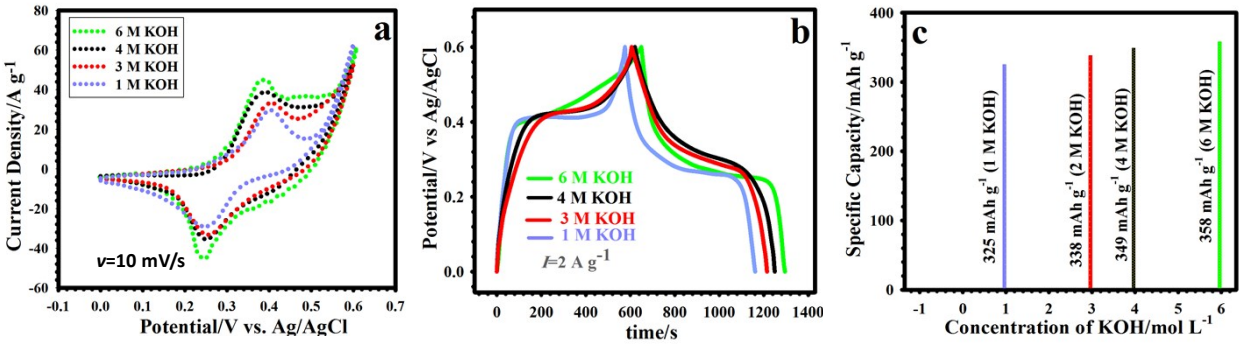

Fig. S2. CV curves of the optimized ZMNS@NSe electrode at 10 mV/s in various concentration of KOH electrolyte. (b) GCD plots of the optimized ZMNS@NSe electrode at 2 A/g in various concentration of KOH electrolyte. (c) The estimated capacity of the optimized ZMNS@NSe electrode in various concentration of KOH electrolyte at 2 A/g.

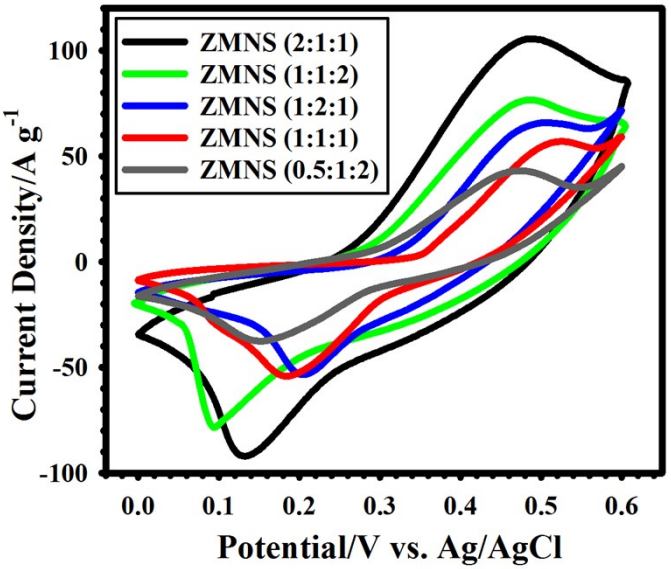

Fig. S3. CV curves of the ZMNS electrode at 60 mV/s in various molar ratios.

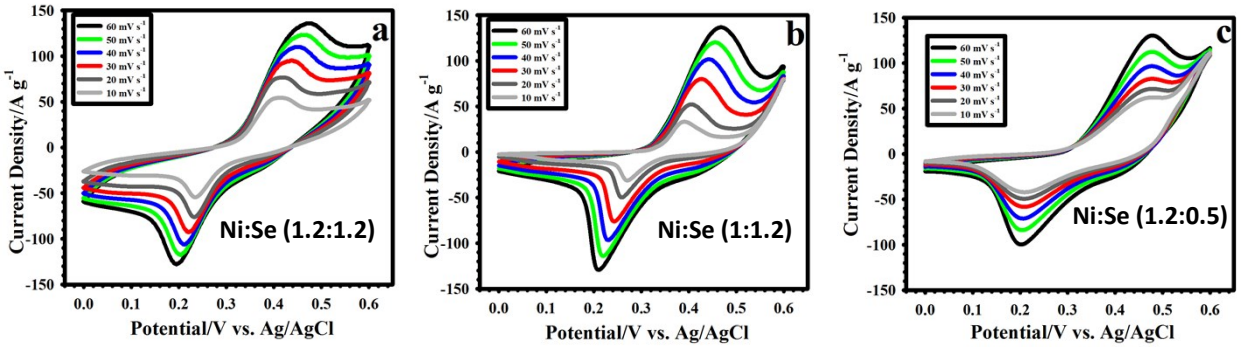

Fig. S4. (a-c) CV curves of the ZMNS@NSe electrode with several mmol ratios of the $NiCl_2.6H_2O$: SeO_2 at different sweep speeds.

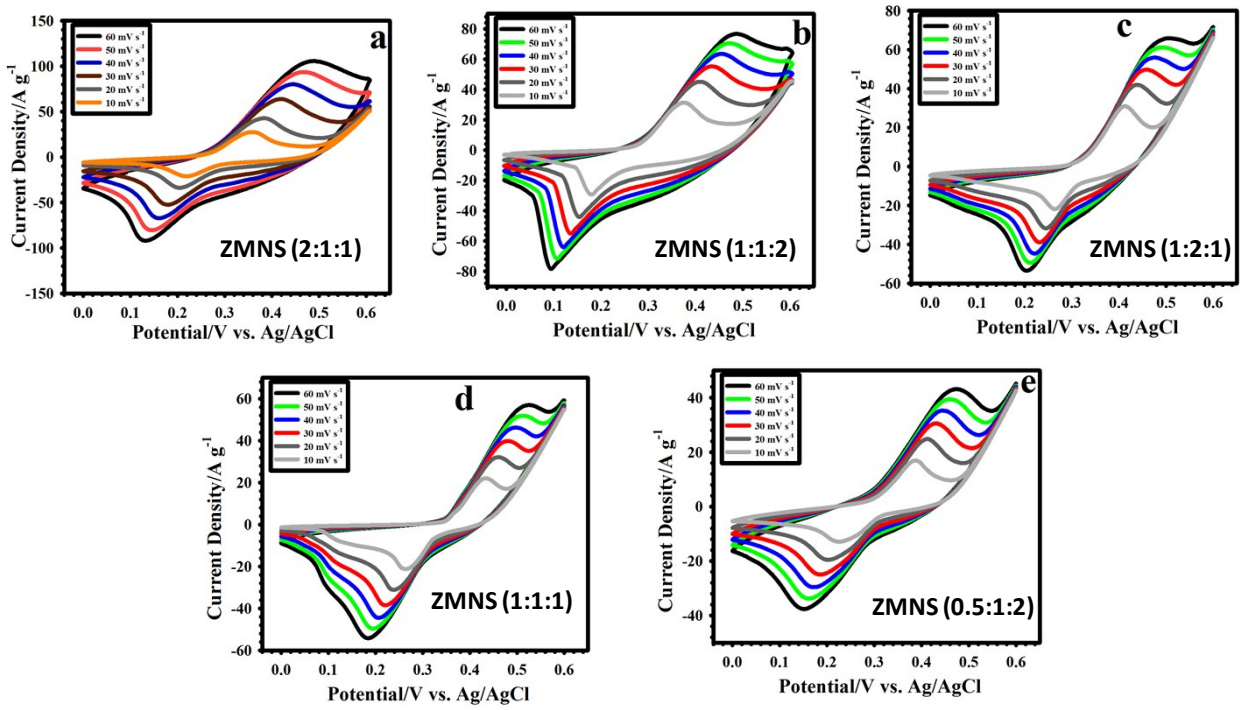

Fig. S5. (a-e) CV curves of the ZMNS electrode with various molar ratios at different sweep speeds.

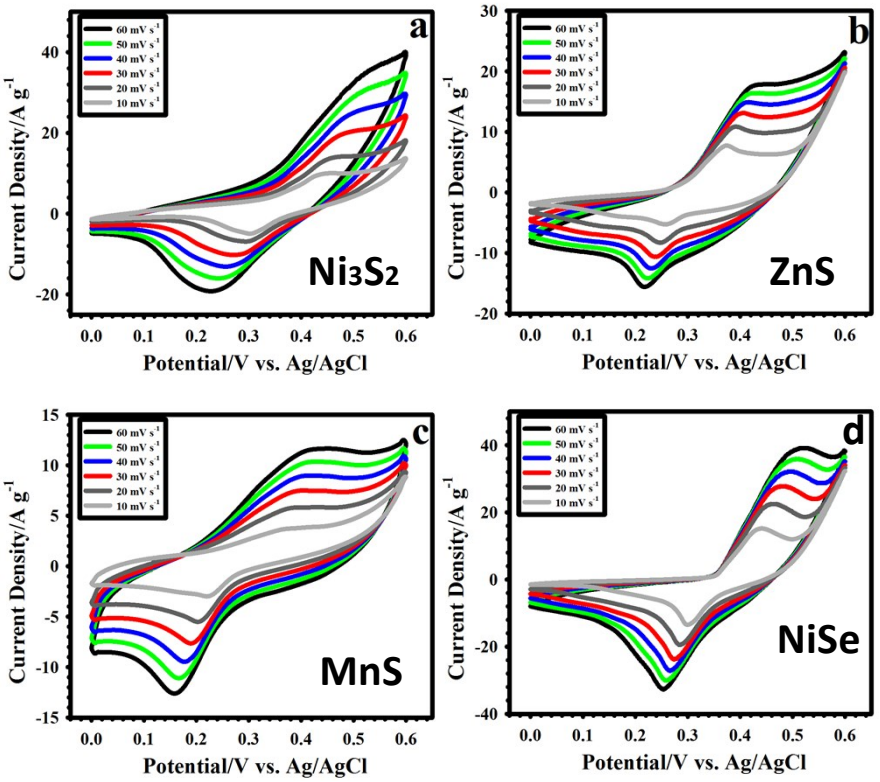

Fig. S6. CV curves of the (a) Ni_3S_2, (b) ZnS, (c) MnS, and (d) NiSe electrodes at different sweep speeds.

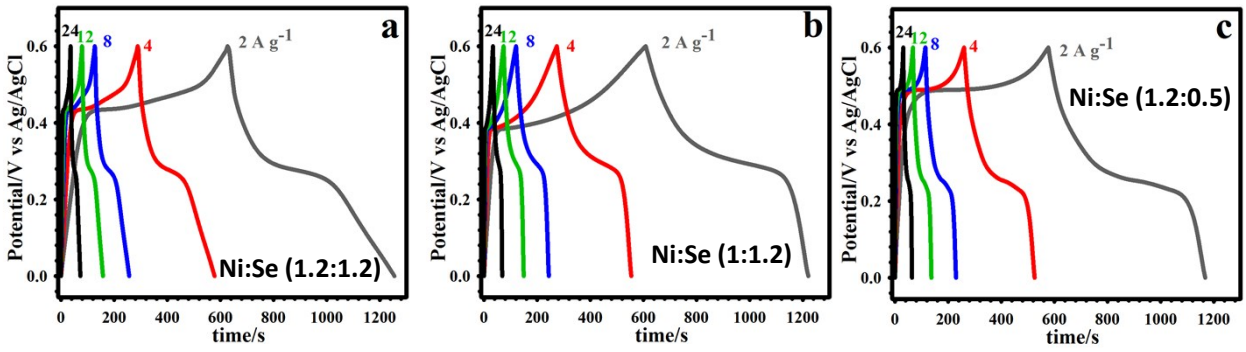

Fig. S7. (a-c) GCD plots of the ZMNS@NSe electrode with several mmol ratios of the $NiCl_2.6H_2O$: SeO_2 at different current densities.

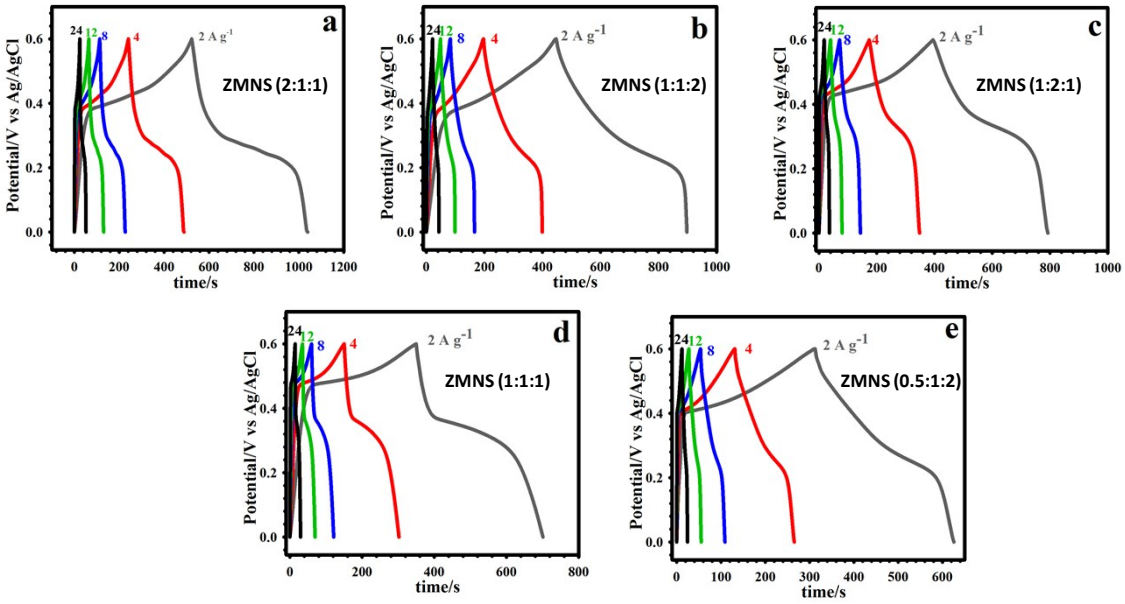

Fig. S8. (a-e) GCD plots of the ZMNS electrode with various molar ratios at different current densities.

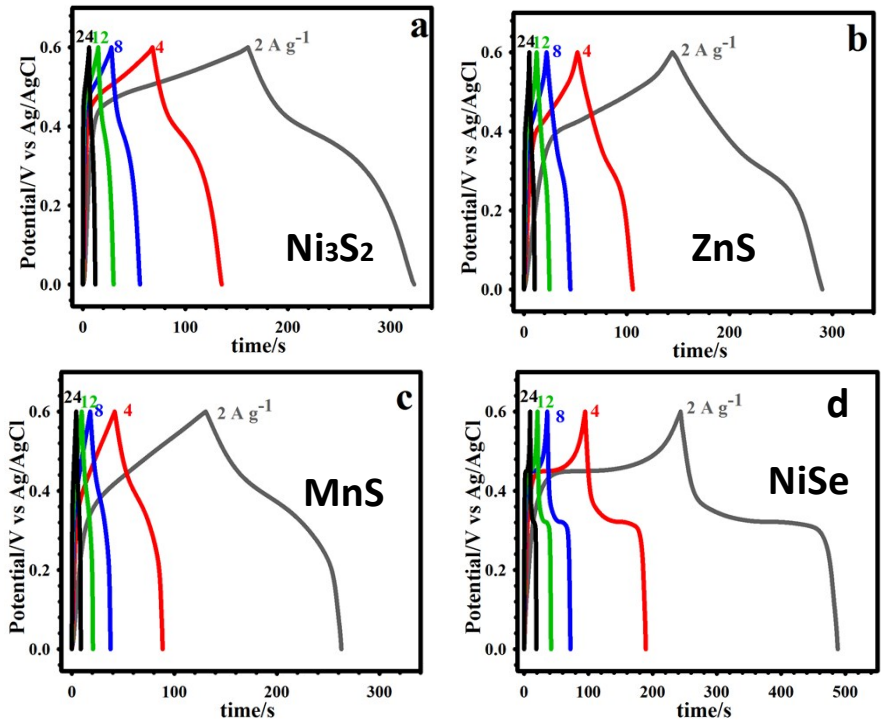

Fig. S9. GCD plots of the (a) Ni_3S_2, (b) ZnS, (c) MnS, and (d) NiSe electrodes at different current densities.

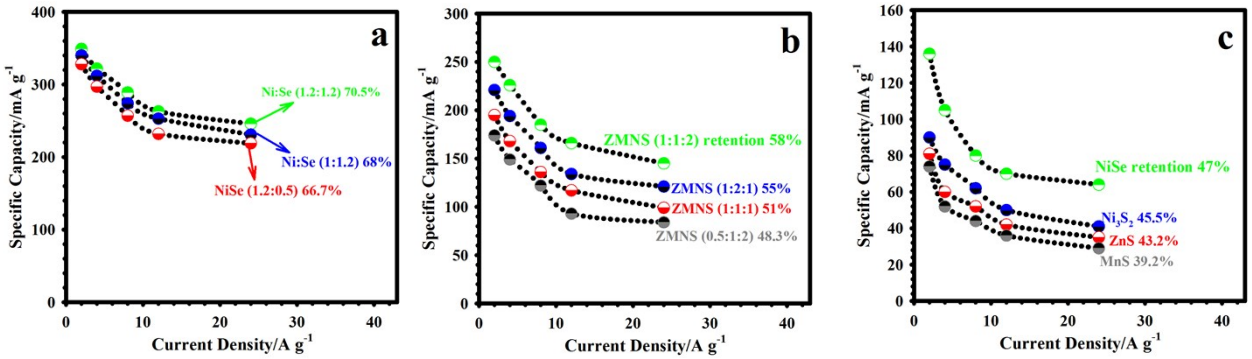

Fig. S10. (a) Rate capability of the ZMNS@NSe with several mmol ratios of the $NiCl_2.6H_2O$: SeO_2 (b), Rate capability of the ZMNS with various molar ratios. (c) Rate capability of the NiSe, Ni_3S_2, ZnS, and MnS electrodes.

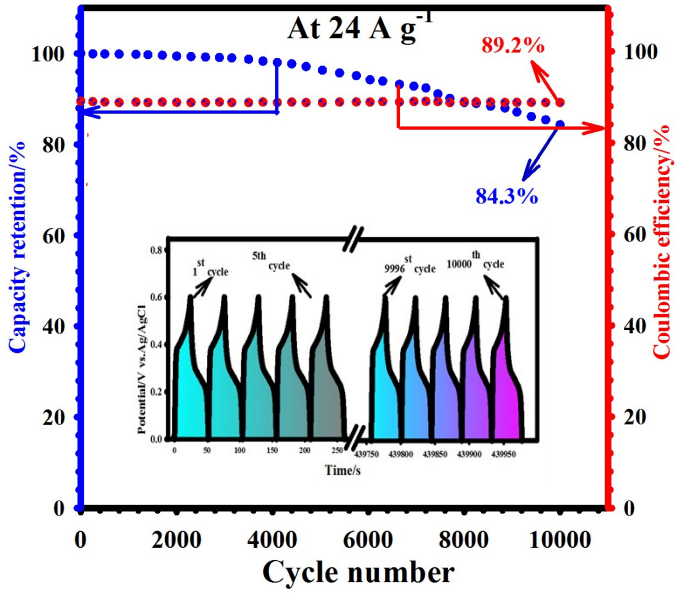

Fig. S11. The durability and Coulombic efficiency of the optimized ZMNS electrode at 24 A g^{-1} (the inset presents the first and last five GCD cycles).

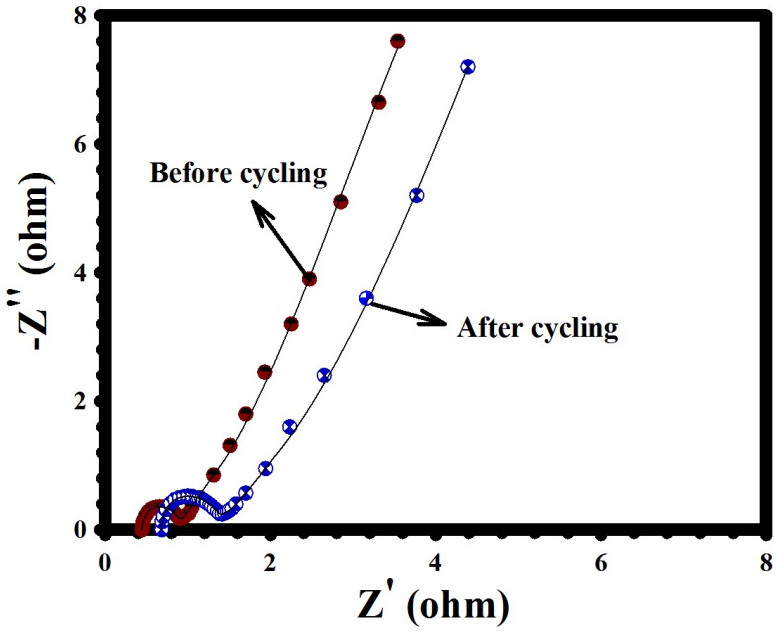

Fig. S12. Nyquist graphs of the optimized ZMNS before and after cycling.

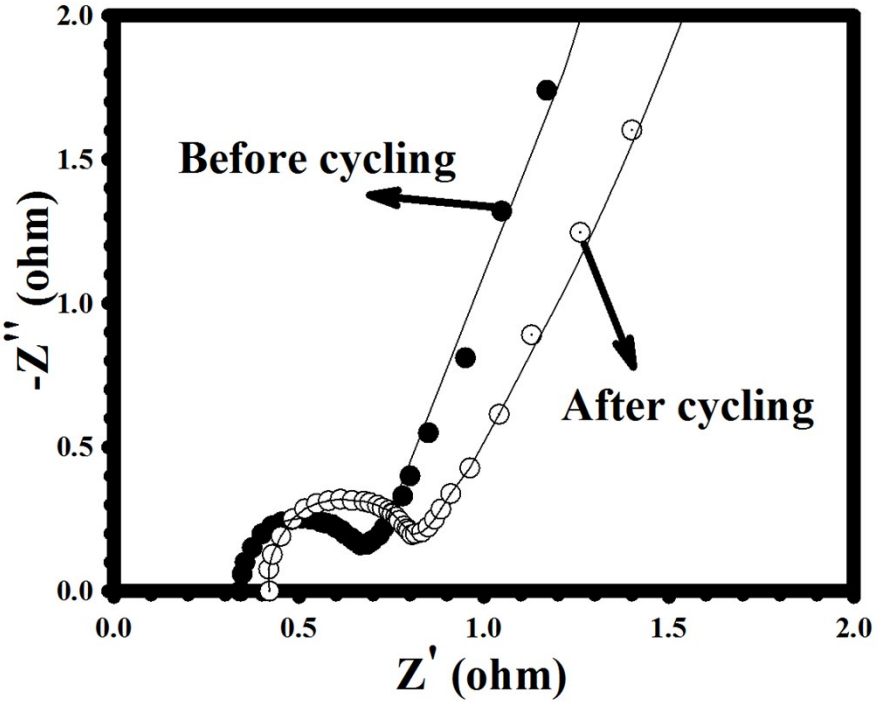

Fig. S13. Nyquist graphs of the optimized ZMNS@NSe before and after cycling.

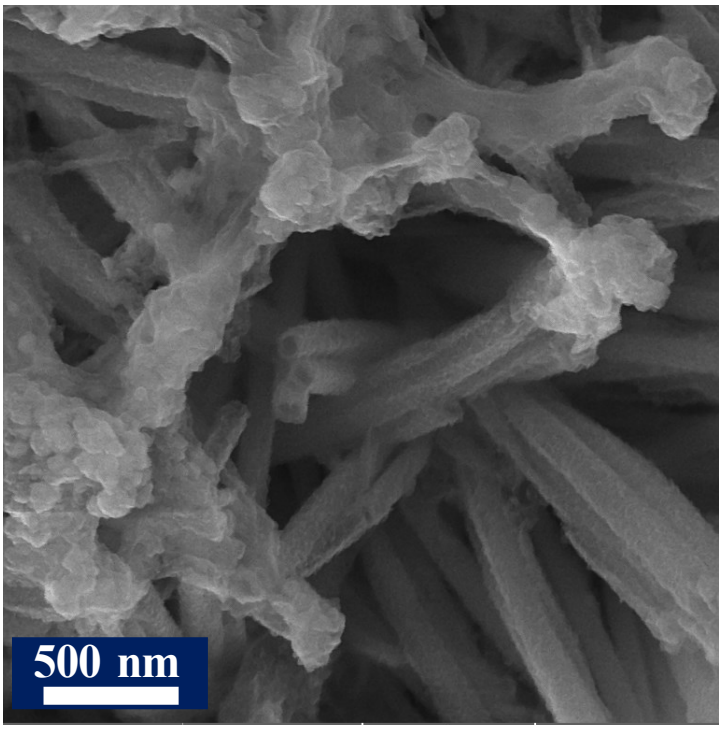

Fig. S14. FE-SEM image of the optimized ZMNS electrodes after cycling.

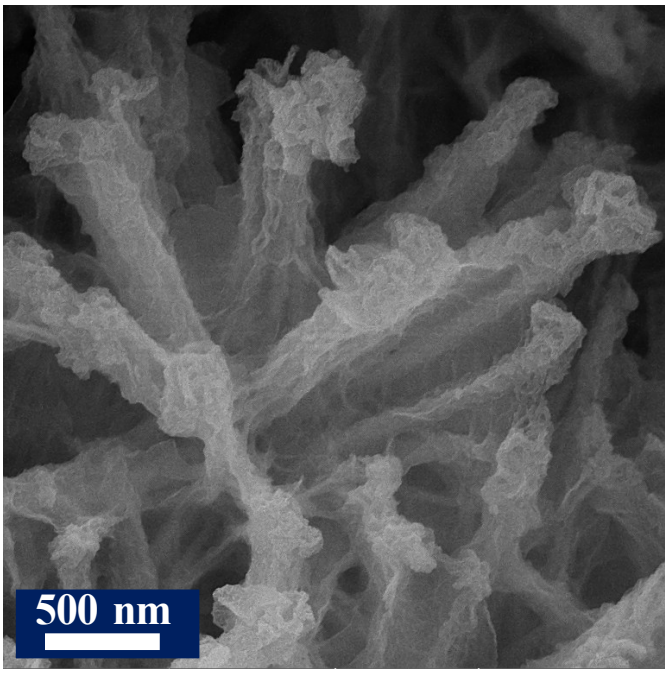

Fig. S15. FE-SEM of the optimized ZMNS@NSe after cycling.

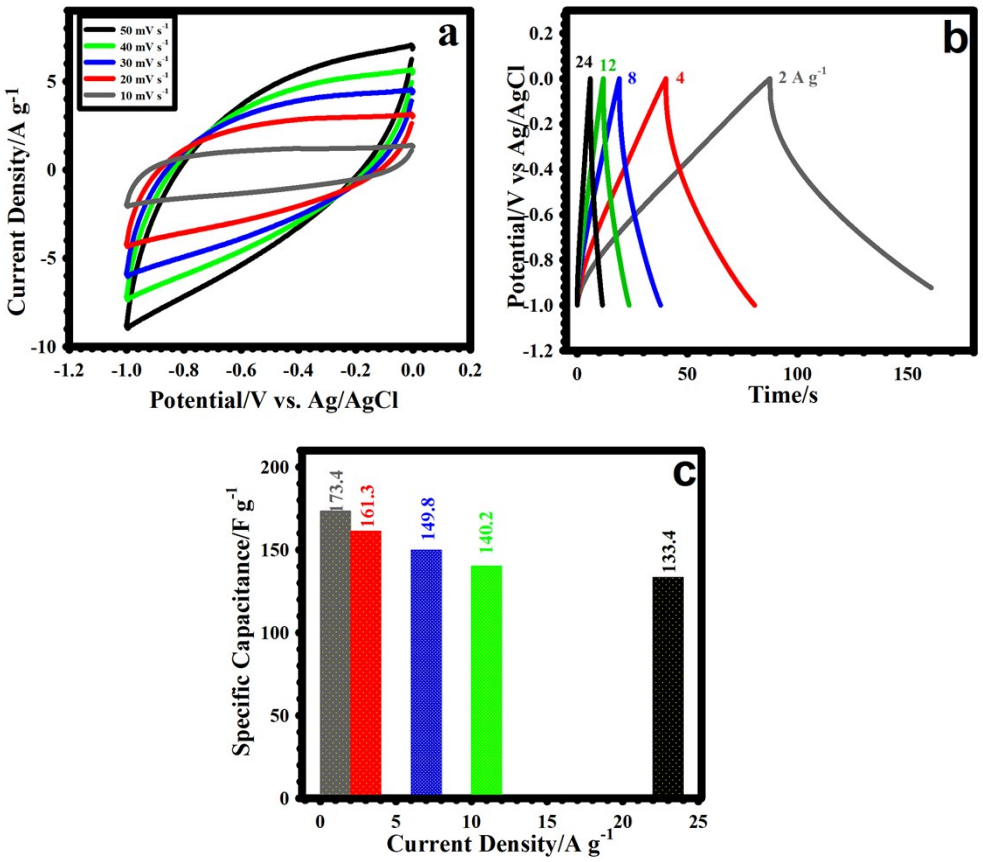

Fig. S16. (a) CV curves of the AC electrode at different sweep rates. (b) GCD profiles of the AC electrode at miscellaneous current densities. (c) Rate capability of the AC electrode.

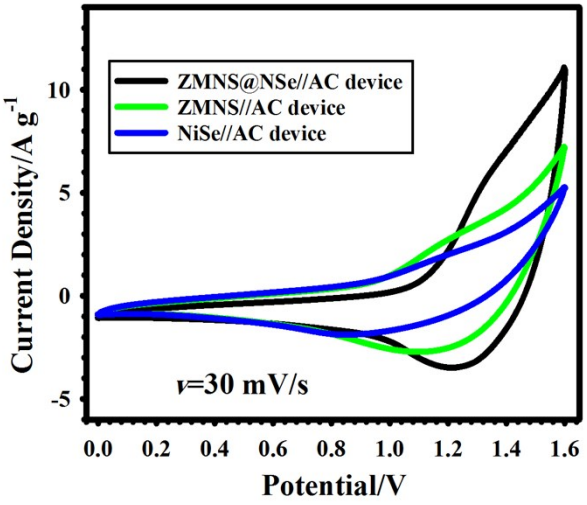

Fig. S17. CV curves of the ZMNS@NSe//AC, ZMNS//AC, and NiSe//AC at 30 mV/s.

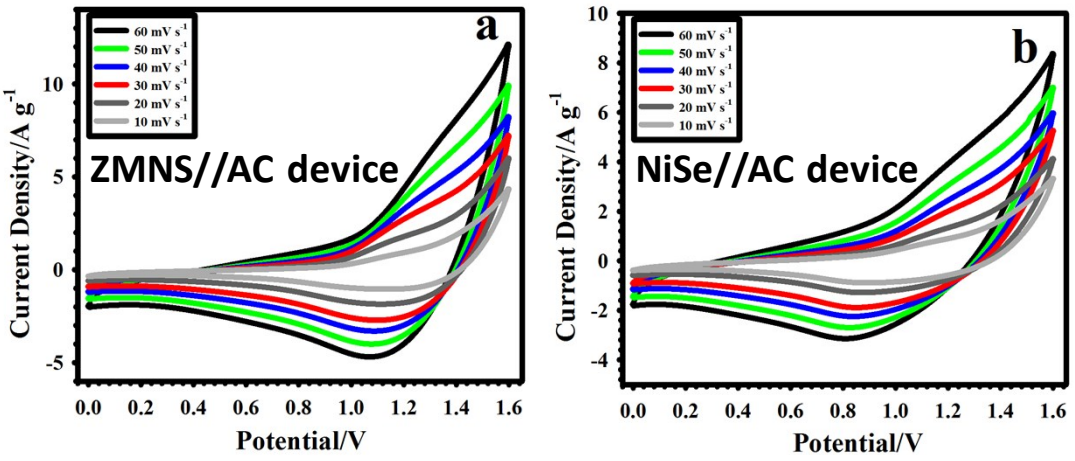

Fig. S18. (a) CV curves of the ZMNS//AC device at various scan rates. (b) CV curves of the NiSe//AC device at various scan rates.

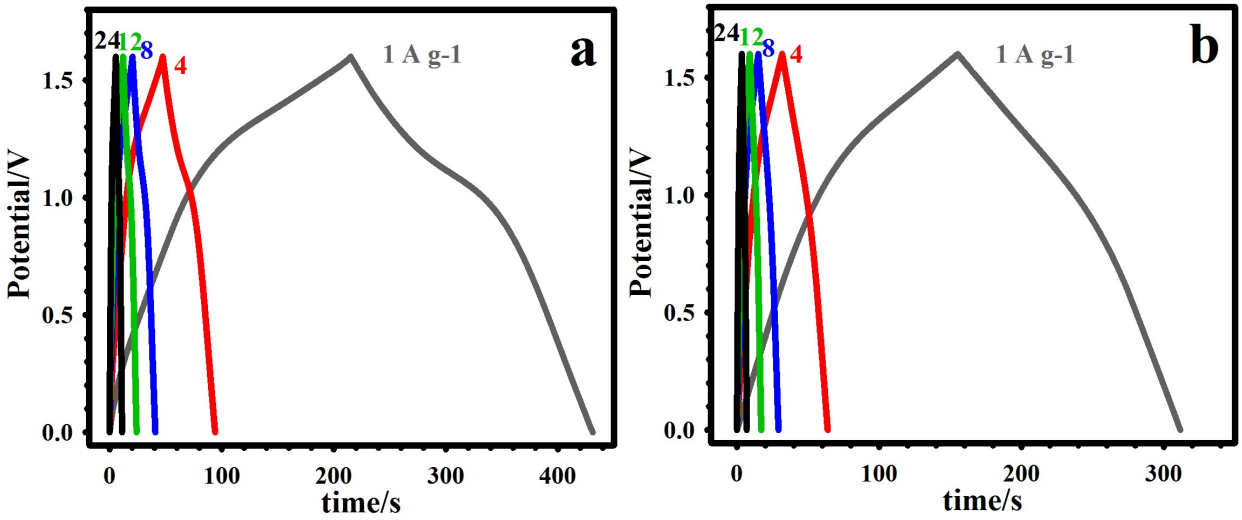

Fig. S19. (a) GCD plots of the ZMNS//AC device at various current densities. (b) GCD plots of the NiSe//AC device at various current densities.

Table S1. Comparison of the electrochemical performance of the optimized ZMNS@NSe electrode in three and two electrode systems with other previously reported electrodes.

Composition	*Capacity/capacitance 3 and 2 electrodes (mAh g^{-1}, F g^{-1})*	Cycles, retention 2 and 3 electrode	ED (W h kg^{-1}) 2 Electrode	Reference
$W0_{.4}Mo_{0.6}O_3$	115.7 mAh g^{-1} at 1 A g^{-1} (3 E)	2000, 82.3% (2 E)	20.2	1
T-Nb_2O_5@Ni_2P	105 mAh g^{-1} at 1 A g^{-1} (3 E)	5000, 90% (2 E)	30.2	2
$MnCo_2O_{4.5}$@$Ni(OH)_2$	318 mAh g^{-1} at 3 A g^{-1} (3 E)	5000, 87.3% (3 E) 3000, 90.4% (2 E)	56.53	3
SDBS-$Ni_2Co_1PO_4$	191.6 mAh g^{-1} at 1 A g^{-1} (3 E)	2000, 77% (3 E) 2000, 76% (2 E)	36.5	4
Ni_2P-CNFs	145 mAh g^{-1} at 1 A g^{-1} (3 E)	6000, 88% (2 E)	42	5
Co_3O_4/$Co(OH)_2$	184.9 mAh g^{-1} at 1 A g^{-1} (3 E)	5000, 90% (3 E) 5000, 91% (2 E)	37.6	6
Co-Cd-Se	192 mAh g^{-1} at 1 A g^{-1} (3 E)	1000, 95.2% (3 E) 1000, 80.9% (2 E)	57.6	7
ZMNS@NSe	**358 mAh g^{-1} at 2 A g^{-1} (3 E)**	**10000, 90.1 (3 E)** **10000, 86.6 (2 E)**	**59.6**	**This work**

References

1 H. Peng, S. Cui, X. Xie, G. Wei, K. Sun, G. Ma and Z. Lei, *Electrochim. Acta* 2019, **322**, 134759.

2. F. Wang, H. Lei, H. Peng, J. Zhou, R. Zhao, J. Liang, G. Ma and Z. Lei, *Electrochim. Acta* 2019, **325**, 134934.

3. Y.-L. Liu, C. Yan, G.-G. Wang, H.-Y. Zhang, L.-Y. Dang, B.-W. Wu, Z.-Q. Lin, X.-S. An and J. Han, *ACS Appl. Mater. Interfaces* 2019, **11**, 9984-9993.

4. X. Zhang, N. Shang, S. Gao, C. Wang, Y. Gao and Z. Wang, *Appl. Surf. Sci.* 2019, **483**, 529-535.

5. H. Peng, J. Zhou, Z. Chen, R. Zhao, J. Liang, F. Wang, G. Ma and Z. Lei, *J. Alloys Compd.* 2019, **797**, 1095-1105.

6 G. Lee and J. Jang, *J. Power Sources* 2019, **423**, 115-124.

7 Z.-B. Zhai, K.-J. Huang and X. Wu, *Nano Energy,* 2018*,* **47**, 89-95.